JOURNAL OF VIROLOGY, Apr. 1996, p. 2556–2561 Vol. 70, No. 4
0022-538X/96/$04.00+0

Suppression of Long-Distance Movement of Tobacco Etch Virus in a Nonsusceptible Host

MARY C. SCHAAD AND JAMES C. CARRINGTON*

Department of Biology, Texas A&M University, College Station, Texas 77843

Received 25 August 1995/Accepted 18 December 1995

To investigate host functions involved in the tobacco etch potyvirus (TEV) infection process, a tobacco line (V20) with a strain-specific defect in supporting systemic infection was analyzed. Using a modified TEV encoding a reporter protein, β-glucuronidase (GUS), genome amplification, cell-to-cell movement, and long-distance movement were measured in V20 and a susceptible line, Havana425. Comparable levels of TEV-GUS genome amplification were measured in inoculated protoplasts from both tobacco lines. The rates of cell-to-cell movement of virus in inoculated leaves were nearly identical in V20 and Havana425 between 48 and 72 h postinoculation. In contrast, long-distance movement from leaf to leaf was markedly restricted in V20 relative to Havana425. In situ histochemical analysis of inoculated leaves revealed that infection foci expanded radially over time, providing the potential for contact of virus with veins. Immunocytochemical analysis of V20 tissue from infection foci indicated that TEV-GUS entered the phloem parenchyma or companion cells adjacent to the sieve elements, suggesting that the block in long-distance movement was associated with entry into, or exit from, sieve elements. The genetic basis for the V20 restriction was characterized in a segregation analysis of a cross between V20 and Havana425. The heterozygous F_1 progeny displayed the susceptible phenotype, indicating that the V20 restriction was a recessive trait. Segregation in the F_2 progeny indicated that the restriction was likely due to the interaction of recessive genes at two nonlinked loci. These data support the hypothesis that long-distance movement requires a set of host functions that are distinct from those involved in cell-to-cell movement.

Systemic infection of plants by viruses requires compatible interactions between viral and cellular factors. Viruses must first replicate in the initially infected cells and then move to adjacent cells through plasmodesmata (27). In the case of tobacco etch potyvirus (TEV), this results in radially expanding foci in inoculated leaves (12, 14). Cell-to-cell movement to phloem parenchyma and companion cells, followed by entry into sieve elements, is required for long-distance transport to other organs and tissues (19, 25). The virus must then exit from sieve elements and establish replication and cell-to-cell movement activities in distal tissues.

Many viruses encode movement proteins (MPs) that facilitate cell-to-cell movement through plasmodesmata (8, 10). Depending on the virus, MPs promote movement by a variety of mechanisms. In some cases, MPs bind directly to the viral genome and interact with the plasmodesmata, whereas in some other cases, MPs form intercellular tubules through which entire virions pass. A dedicated MP has not been identified with TEV, although cell-to-cell movement functions have been mapped to the capsid protein (CP). Mutational analysis revealed that the CP core domain (amino acids 30 to 247 within the 263-amino-acid CP) is essential for both cell-to-cell movement and assembly of filamentous virions (12, 13).

The requirements for long-distance movement through the phloem differ from the requirements for cell-to-cell movement. For some viruses, CPs as well as MPs are required for efficient long-distance movement (19). Proteins involved in genome replication also have been shown to affect the efficiency of long-distance movement or accumulation of virus in systemic tissue (11, 15, 18, 33, 37). For TEV, the surface-oriented amino and carboxyl regions of CP are not required for cell-to-cell movement but are required for long-distance movement (12, 13). The central region of the helper component-proteinase (HC-Pro) is also required for long-distance movement (9). Sequence changes introduced into these regions result in mutants that are capable of assembly and cell-to-cell movement but not long-distance movement. It has been proposed that HC-Pro interacts with CP, as either a virion or nonvirion ribonucleoprotein, to form active transport complexes capable of long-distance movement (9). Indirect evidence for an interaction between HC-Pro and virions has been presented (2).

The nature of the host factors that interact with these, and possibly other, viral proteins in active transport complexes is unknown. Host factors may be involved in intracellular transport to plasmodesmata or may be proteins specifically associated with plasmodesmata. We have begun a genetic study to examine host factors required for these interactions. In this report, a tobacco mutant (V20) containing recessive genes that suppress long-distance movement of TEV is described.

MATERIALS AND METHODS

Virus strains and plant lines. The highly aphid transmissible (HAT) strain and the Oxnard strain of TEV were used for these studies. A modified form of TEV-HAT, represented as cDNA in pTEV7DAN-GUS, was also used. The virus derived from transcripts of this plasmid encodes the reporter protein β-glucuronidase (GUS) and is termed TEV-GUS (14). Three *Nicotiana tabacum* lines were used: Xanthi nc, Havana425 and V20 (7). The V20 seed was obtained from Richard Christie, University of Florida.

Inoculation of plants and protoplasts. Carborundum-dusted plants were inoculated mechanically with extracts prepared by grinding 1 g of virus-infected leaves in 5 ml of TE buffer (10 mM Tris-HCl [pH 7.6], 1 mM EDTA). In some experiments, immunoblot analyses were conducted with anticapsid serum as in previous studies (29). Protoplasts (7.5×10^5) were inoculated with transcripts (10 μg) synthesized in vitro with SP6 RNA polymerase, using *Bgl*II-linearized plasmid pTEV7DAN-GUS or pTEV7DAN-GUS/VNN as described previously (6, 28). Transcripts derived from pTEV7DAN-GUS/VNN were RNA amplification defective as a result of a substitution mutation that inactivated NIb polymerase (26).

GUS activity assays. Protoplasts (2.5×10^5) were harvested at 24, 48, and 72

* Corresponding author. Phone: (409) 845-2325. Fax: (409) 845-2891. Electronic mail address: carrington@bio.tamu.edu.

h postinoculation (p.i.). Cells from a portion of each sample were bound to nitrocellulose and incubated with the colorimetric GUS substrate 5-bromo-4-chloro-3-indolyl-β-D-glucuronide (X-gluc). The number of protoplasts that reacted with the substrate was divided by the total number of protoplasts to determine the percentage of cells that were infected. Cells from the remaining portion of each sample were frozen at −80°C, thawed, and resuspended in GUS lysis buffer (40 mM sodium phosphate, 10 mM EDTA, 0.1% Triton X-100, 0.1% sodium lauryl sarcosine, 0.07% β-mercaptoethanol [pH 7.0]). GUS activity was measured by using the fluorometric substrate 4-methylumbelliferyl-β-D-glucuronide (21). Activity values were calculated as picomoles of substrate cleaved per minute per 10^5 protoplasts.

Tissue from leaves that were either two nodes (2+) or three nodes (3+) above the inoculated leaf was ground in 5 volumes of GUS lysis buffer and clarified by centrifugation at 13,000 × *g* for 1 min. GUS activity was measured by using the fluorometric substrate 4-methylumbelliferyl-β-D-glucuronide. Total protein concentration was determined by the method of Bradford (5). Activity values were calculated as picomoles of substrate cleaved per minute per microgram of protein.

GUS activity was visualized in inoculated leaves after vacuum infiltration of the colorimetric substrate X-gluc (21). Infection focus diameter was measured at 24, 48, 72, and 96 h p.i. as described previously (12).

Immunochemistry and microscopy. Inoculated leaves of tobacco plants were infiltrated with X-gluc at 6 days p.i. Tissue near the edge of an infection focus was excised and fixed in 50 mM piperazine-*N*,*N*′-bis(2-ethanesulfonic acid) (PIPES; pH 7.4)–4% paraformaldehyde (Electron Microscopy Sciences)–0.5% glutaraldehyde (Sigma). After fixation, the samples were dehydrated through a 10-30-50-70-90% acetone series for 30 min at each step, followed by infiltration with 25, 50, 75, and 100% Historesin (Reichert-Jung) for 1 h at each step at room temperature. After polymerization of the Historesin, 6-μm sections were cut with a Reichert Ultracut microtome and placed on poly-L-lysine-coated glass slides. For immunolocalization of CP, the sections were incubated with blocking buffer (1× phosphate-buffered saline [PBS; pH 7.2], 1% bovine serum albumin, 0.05% sodium azide, 5% sheep serum, 5% dry milk) for 1 h. Sections were incubated for 30 min in primary antibody (anticapsid or preimmune) diluted 1:100 in blocking buffer. The slides were rinsed with filtered PBST (1× PBS, 0.05% Tween) and then incubated with secondary antibody (Cy3-conjugated sheep anti-rabbit immunoglobulin G; Sigma) diluted 1:200 in blocking buffer. Slides were rinsed with filtered PBST followed by filtered deionized water. SlowFade Light and equilibration buffer (Molecular Probes, Inc.) were added to the slides, and coverslips were applied. Bright-field and fluorescence microscopy was conducted with an Olympus BX50 microscope. The Cy3 fluorochrome was detected with the DM570 dichroic mirror/BP530-550 exciter filter/BA590 barrier filter set.

Genetic analysis. The stigmas from immature flowers of Havana425 were dusted with pollen from V20 plants. Seeds from crossed plants were germinated, and the resulting heterozygous F_1 plants were allowed to self-fertilize to produce the F_2 seed. One-hundred eighty-seven F_2 seeds (from one F_1 plant) were germinated, and the plants were inoculated with TEV-GUS. The systemic infection phenotype of each plant was determined by appearance of visual symptoms and GUS activity in 2+ leaves. From all plants that tested negative for systemic infection, an inoculated leaf was infiltrated with X-gluc substrate to visualize initial infection foci. The statistical fit between the observed segregation of phenotypes and predicted Mendelian genotypic ratios was determined by a chi-square frequency test.

RESULTS

Systemic infection of TEV-HAT, but not TEV-Oxnard, is restricted in V20. It was reported previously that the V20 line of tobacco is resistant to most, but not all, strains of TEV (7). V20 was found to be susceptible to one strain, formerly designated TEV-6 and currently known as TEV-Oxnard. Havana425 and V20 tobacco plants were inoculated with TEV-HAT and TEV-Oxnard, and systemic infectivity was tested by immunoblot analysis with anticapsid serum at 7 days p.i. Only tissue from 2+ leaves was used. Capsid protein was detected in Havana425 plants infected with either isolate (Fig. 1, lanes 6 and 12). In contrast, CP was detected in the V20 plants inoculated with TEV-Oxnard (lanes 7 to 11) but not with TEV-HAT (lanes 1 to 5).

The genome of the HAT strain of TEV was modified previously by insertion of the GUS coding sequence (14). TEV-GUS exhibited a restricted phenotype in V20 that was similar to that of TEV-HAT and was used in all subsequent experiments.

TEV-GUS amplifies to comparable levels in V20 and Havana425 protoplasts. The suppression of systemic infection in

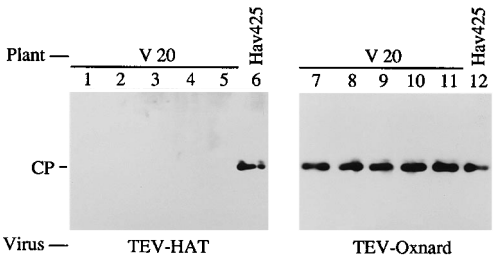

FIG. 1. Immunoblot analysis of TEV-HAT- and TEV-Oxnard-infected V20 and Havana425 plants. Total sodium dodecyl sulfate-soluble proteins were extracted at 7 days p.i. from systemic leaves two positions above the inoculated leaves and subjected to immunoblot analysis with anticapsid serum. The electrophoretic position of CP is indicated.

V20 could be due to restriction of genome amplification at the single-cell level, restriction of cell-to-cell movement, or restriction of long-distance movement. To measure genome amplification at the single-cell level, V20 and Havana425 protoplasts were inoculated with RNA transcripts representing the TEV-GUS genome, and GUS activity was measured at 24, 48, and 72 h p.i. Additionally, the proportion of cells infected after each inoculation was determined by using an in situ histochemical assay. The GUS activity assay has proven to be a sensitive, quantitative measure of genome amplification efficiency (26, 30, 36).

By using two independent protoplast preparations from each tobacco line, TEV-GUS was amplified in both V20 and Havana425 cells, whereas the replication-defective VNN mutant failed to show any appreciable increase in GUS activity in cells from either line (Fig. 2). The TEV-GUS-induced activity levels (picomoles per minute per 10^5 protoplasts) were approximately three to seven times higher in Havana425 than in V20 (Table 1). However, the percentage of inoculated cells that were actually infected differed between the two lines. While an average of 3.1% of the Havana425 cells were infected, only 1.2% of the V20 cells on average were infected. The average GUS activity per infected cell was calculated to be 0.36 ± 0.07 pmol/min for V20 and 0.58 ± 0.04 pmol/min for Havana425 (Table 1). Therefore, V20 protoplasts supported TEV-GUS

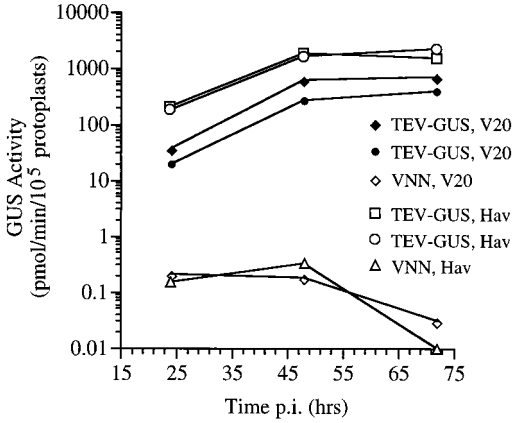

FIG. 2. Amplification of TEV-GUS in V20 and Havana425 protoplasts. GUS activity was measured in protoplasts inoculated with TEV-GUS or VNN mutant transcripts at 24, 48, and 72 h p.i. The experiment was conducted with two independent protoplast preparations from both V20 (●, ◆) and Havana425 (Hav; □, ○). Data from one V20 and one Havana425 protoplast preparation inoculated with VNN transcripts are shown (△, ◇). All datum points represent the mean of two replicate samples for each protoplast preparation.

TABLE 1. Amplification of TEV-GUS in V20 and Havana425 protoplasts

Protoplast prep[a]	GUS activity (U)/10^5 protoplasts[b]	% of protoplasts infected[c]	GUS activity (U)/ infected protoplast
V20-1	621	1.43	0.43
V20-2	265	0.94	0.28
Avg, V20	443	1.19	0.36
Hav425-1	1,900	3.08	0.61
Hav425-2	1,673	3.10	0.54
Avg, Hav425	1,787	3.09	0.58

[a] Two independent protoplast preparations for both V20 and Havana425 (Hav425) were tested at 48 h p.i.

[b] One unit of GUS activity = 1 pmol of substrate cleaved per min per 10^5 protoplasts.

[c] Calculated as 100 × (number of cells containing GUS activity/total number of cells). The numbers of cells sampled were as follows: V20-1, 1,812; V20-2, 1,390; Hav425-1, 1,267; and Hav425-2, 1,456.

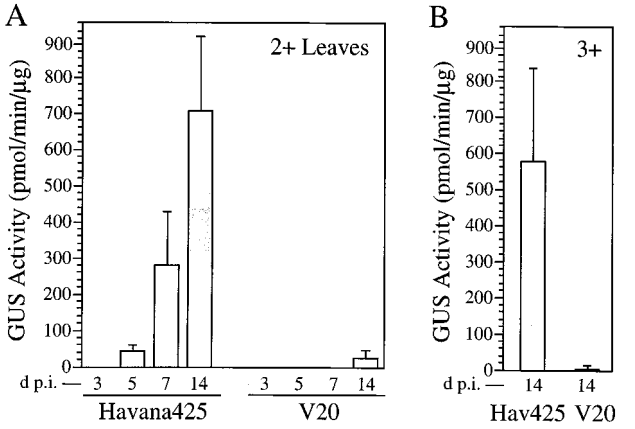

FIG. 4. Systemic infection of Havana425 and V20 plants by TEV-GUS. GUS activity was quantitated in 2+ (A) and 3+ (B) leaves at various days (d) p.i. Each bar represents the mean (± standard deviation) from 10 plants.

amplification to an average of 62% of the level supported by Havana425.

V20 supports cell-to-cell movement of TEV-GUS. To determine cell-to-cell movement rates of TEV-GUS in Havana425 and V20, inoculated leaves were vacuum infiltrated with X-gluc at 24, 48, 72, and 96 h p.i., and the diameters of at least 50 infection foci were determined microscopically at each time point (Fig. 3). With this approach, it is possible to measure infection foci consisting of as few as one epidermal cell (12–14). At 24 h p.i., most foci in Havana425 consisted of single cells (average, 1.32 ± 0.59 cells). The Havana425 infection foci expanded at a rate of 0.17 cells per h between 24 and 72 h p.i. and at a slightly faster rate between 72 and 96 h p.i. Infection foci in V20 were not detected until 48 h p.i. Between 48 and 96 h p.i., however, infection foci in V20 expanded at a rate of 0.16 cells per h. Therefore, except for a possible delay in establishment of detectable infection sites, the rate of cell-to-cell movement of TEV-GUS in V20 was not restricted.

V20 restricts long-distance movement of TEV-GUS. Systemic infection of TEV-GUS in Havana425 and V20 plants was measured by using GUS activity assays with extracts from 2+ and 3+ leaves at 3, 5, 7 and 14 days p.i. All of the Havana425 plants were systemically infected by 5 days p.i. (Fig. 4A). In contrast, GUS activity was not detected in systemic tissue of V20 plants until 14 days p.i. At this time point, GUS activity in the 2+ systemic leaves was 30-fold greater in the Havana425 plants than in the V20 plants (Fig. 4A). Only 3 of 16 V20 plants contained detectable GUS activity in systemic leaves, although all V20 plants contained infection foci in inoculated leaves. In the 3+ systemic leaves, this difference was 151-fold (Fig. 4B). These results indicated that the V20 line markedly restricted systemic infection by TEV-GUS.

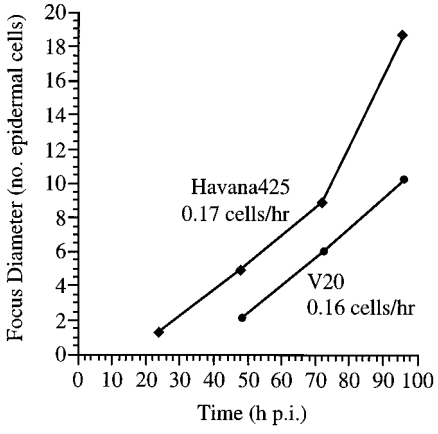

FIG. 3. Cell-to-cell movement of TEV-GUS in Havana425 and V20 plants. Inoculated leaves were infiltrated with X-gluc substrate at 24, 48, 72, and 96 h p.i. and examined microscopically. The diameters (expressed as number of epidermal cells) of at least 50 infection foci per treatment were determined at each time point. The rate of cell-to-cell movement was calculated for the period between 24 and 72 h p.i. for Havana425 and for the period between 48 and 96 h p.i. for V20.

Several possible mechanisms could account for the inhibition of long-distance movement of TEV-GUS in V20. The block may have been due to an inability to reach the vasculature in inoculated leaves, an inability to enter the cells within the vascular bundles, or an inability to enter and/or exit the sieve elements. To determine whether TEV-GUS could reach the vasculature, inoculated V20 leaves were infiltrated with the GUS colorimetric substrate at 5, 7, and 14 days p.i. In these experiments, *N. tabacum* Xanthi nc was used as the susceptible control. This tobacco variety is as susceptible to TEV-GUS as is Havana425. By 5 days p.i., TEV-GUS had spread throughout the inoculated Xanthi nc leaves via cell-to-cell and vasculature-associated secondary movement (Fig. 5A). In contrast, TEV-GUS remained confined primarily to initial infection foci in V20 throughout the course of the experiment. By 14 days p.i., some infection foci in V20 had coalesced, and apparent tracking along primary veins was observed. This tracking may have been due either to cell-to-cell movement along veins or to phloem-mediated movement for only short distances. The continued expansion of infection foci through 14 days p.i. in V20 suggests that the long-distance movement suppression was not due to a failure to encounter vascular tissue.

TEV-GUS infects phloem cells in inoculated V20 leaves. To test whether the entry of TEV-GUS into phloem parenchyma or companion cells was restricted, X-gluc-stained tissue from infection foci at 6 days p.i. was embedded in Historesin, cut into 6-μm sections, and examined microscopically. Strong histochemical reactions were detected in mesophyll, bundle sheath, and phloem cells of both Havana425 and V20 (Fig. 5B). The reactions were particularly striking in the cytoplasm-dense phloem cells of both plants. The X-gluc staining was confined to the cytoplasm of these cells, with little leakage of the reaction products into the vacuole. Curiously, sieve elements also appeared to contain blue X-gluc product. The sieve

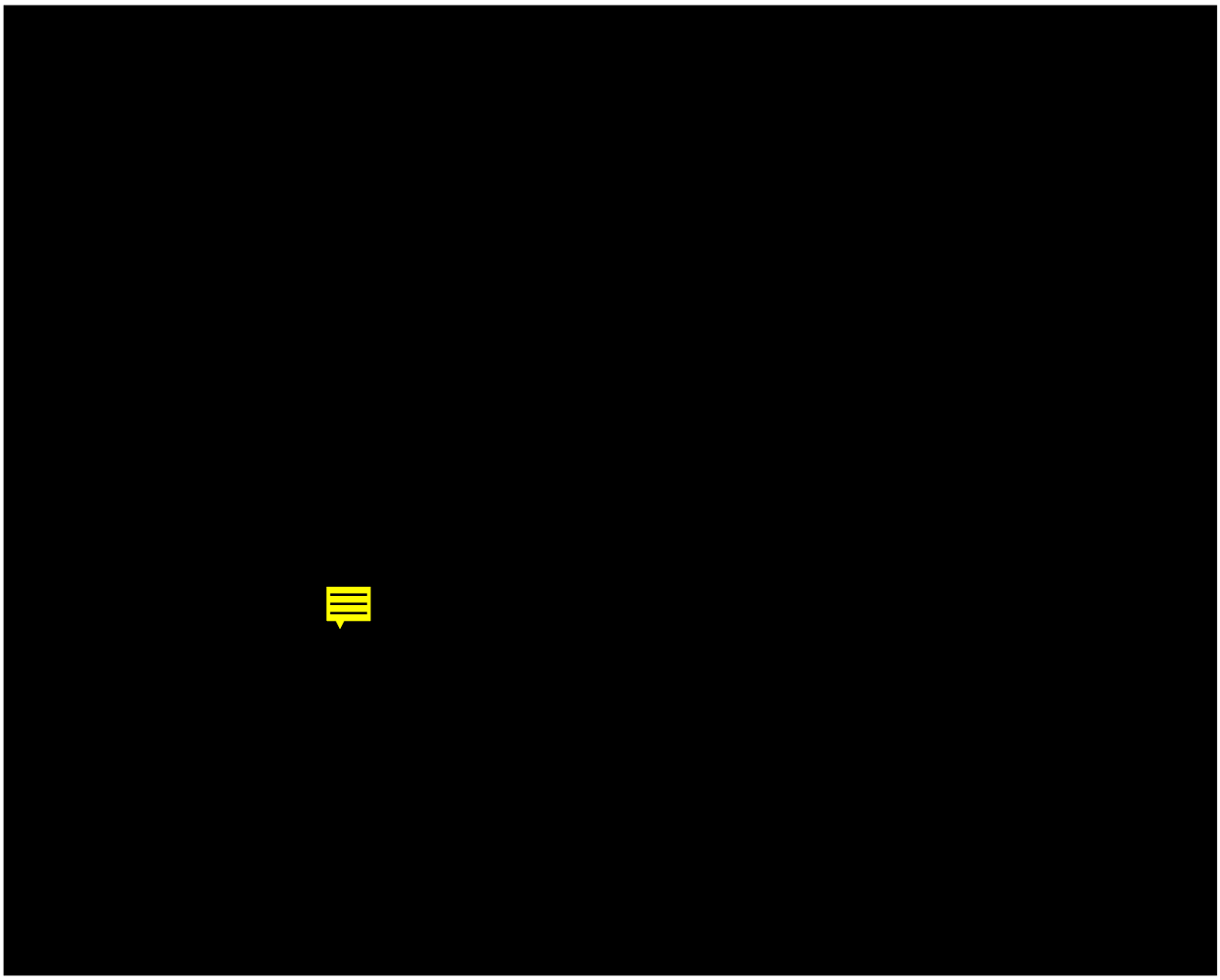

FIG. 5. In situ analysis of TEV-GUS-infected Xanthi nc, Havana425, and V20 plants. (A) Histochemical localization of GUS activity in inoculated leaves of Xanthi nc and V20 at 5, 7, and 14 days (d) p.i. (B) Immunofluorescence microscopy using anticapsid or preimmune serum and Cy3-conjugated second antibody. Inoculated leaf tissue from noninfected V20 or TEV-GUS-infected V20 or Havana425 plants was infiltrated with X-gluc at 6 days p.i. and embedded in Historesin. Six-micrometer sections of tissue containing minor veins are presented. Minor veins, which contain cytoplasm-dense phloem cells surrounding two to three sieve elements, are shown near the center of each micrograph. Xylem elements are located above the phloem. The large cells surrounding the veins are bundle sheath cells. The bright-field micrographs are shown at the top, and the fluorescence micrographs are shown at the bottom. The same field of view is presented in each set of micrographs. In the bright-field micrographs, GUS activity is indicated by the blue color. In the fluorescence micrographs, the capsid antigen is indicated by the punctate, bright red color. Capsid protein-positive phloem cells are indicated by the white arrows. Note that parts of several sections show a slight red color around the xylem walls as a result of autofluorescence. Bar = 14 μm.

element staining may have been due to the actual presence of virus-encoded GUS in the elements or to leakage of the X-gluc product from companion cells. Because of the possibility that the X-gluc product could move between cells, thereby complicating interpretation of the histochemical signal, sections were also subjected to immunofluorescence microscopy using anticapsid or preimmune serum as the first antibody and Cy3-labeled second antibody. No specific immunofluorescence was detected with the preimmune serum, although a slight red autofluorescence was detected from the xylem walls (Fig. 5B). No specific fluorescence was detected in cells of noninfected V20 plants (Fig. 5B). A positive reaction as indicated by bright red, often punctate fluorescence was observed in mesophyll, bundle sheath, and phloem cells of Havana425 and V20 probed with anticapsid serum (Fig. 5B). No consistent differences were observed between the patterns of immunofluorescence with the V20 and Havana425 cells. These results indicate that TEV-GUS is capable of infecting the phloem parenchyma or companion cells in inoculated V20 leaves.

The lack of susceptibility in V20 is due to recessive genes. To characterize the genetic basis for the V20 restriction, a segregation analysis was conducted with a cross between V20 and Havana425. Progeny from the F_1 and F_2 generations, as well as both parents, were inoculated with TEV-GUS and analyzed for systemic infection by the appearance of symptoms or GUS activity in 2+ leaves at 7 days p.i. One hundred percent of the heterozygous F_1 progeny were systemically infected (Table 2), indicating that the susceptible phenotype from Havana425 was a dominant trait. The susceptible and restricted traits segregated in the F_2 progeny. Thirty-four of the 187 F_2 plants (18%) failed to become systemically infected, whereas the remaining 153 plants (82%) were systemically infected (Table 2). This

TABLE 2. Genetic analysis of susceptibility of Havana425 and V20 to TEV

Generation	Plant	Infection phenotype		
		Restricted to inoculated leaves (%)[a]		Systemically infected (%)[b]
		1	2	
P	V20[c]	100	0	0
P	Havana425[d]	0	0	100
F_1	Havana425 × V20[e]	0	0	100
F_2	Havana425 × V20[f]	7.5	10.7	81.8

[a] Plants that restricted virus to inoculated leaves exhibited no symptoms and contained no detectable GUS activity in 2+ leaves at 7 days p.i. Infections fell into one of two categories: (i) restricted to initial foci only and (ii) limited secondary movement along veins of inoculated leaves.

[b] Plants were scored as systemically infected if they exhibited symptoms or if GUS activity was detected in 2+ systemic leaves at 7 days p.i.

[c] $n = 20$.

[d] $n = 20$.

[e] $n = 20$.

[f] $n = 187$.

segregation ratio was statistically different ($P < 0.05$) from the 3:1 Mendelian ratio that would be expected if the susceptible or restricted phenotypes were governed by only a single locus.

To ensure that none of the F_2 plants had escaped infection, and to characterize the pattern of spread of virus within initial infection foci, inoculated leaves of all nonsystemically infected F_2 plants were infiltrated with the X-gluc substrate at 8 days p.i. Each of the 34 nonsystemically infected plants contained virus, although two categories of infection were identified. In category 1, 14 plants (7.5% of total F_2 plants) displayed an infection phenotype identical to that of the V20 parent; that is, virus was restricted to initial foci only. In category 2, 20 plants (10.7%) displayed various degrees of vasculature-associated movement away from the initial foci and therefore represented an intermediate phenotype. In most cases, the limited secondary movement was confined to the inoculated leaf and consisted of spread via one or a few major veins. The observed ratio of category 1 plants to all other plants in the F_2 population was consistent with a segregation ratio expected if the restricted V20 phenotype was due to two nonlinked, recessive loci in the homozygous state ($P > 0.4$).

DISCUSSION

We have shown that the V20 strain of tobacco exhibits a strain-specific defect in supporting systemic infection by TEV. This defect was demonstrated to be a recessive trait conditioned by multiple loci. Through the use of a reporter-tagged virus, TEV-GUS, the major steps in the systemic infection pathway—genome amplification, cell-to-cell movement and long-distance movement—were analyzed in V20 and susceptible control lines.

The ability of V20 cells to support TEV-GUS genome amplification was analyzed by using the protoplast system. Host mutants that restrict virus replication have been characterized in other systems. For example, *Arabidopsis thaliana* carrying the *tom1* mutation supports tobacco mosaic virus (Cg strain) genome replication at a rate much slower than wild-type plants (20). TEV-GUS genome amplification per infected V20 protoplast was measured at 62% of the level of genome amplification per infected Havana425 protoplast. Several TEV mutants, such as those with deletions or substitutions in the P1 or NIa coding sequence, amplify to 0.7 to 20% of the level of parental virus yet infect plants systemically at rates similar to that of the parental virus (31, 35). It is highly unlikely, therefore, that the modest reduction in V20 amplification is sufficient to account for the restricted phenotype.

The rates of TEV-GUS infection focus expansion, which reflect the rate of cell-to-cell movement, were similar in inoculated leaves of V20 and Havana425, although the timing of focus expansion was delayed by approximately 24 h in V20 relative to Havana425. Infection foci continued to expand in V20 over 14 days without any visible host defense responses, resulting in virus movement into epidermal, mesophyll, bundle sheath, and phloem parenchyma/companion cells. The V20 restriction, therefore, cannot be explained merely by an impairment of cell-to-cell movement. Rather, the data suggest that V20 fails to support efficient long-distance movement of TEV-GUS. Vasculature-associated movement throughout the inoculated leaves and to upper, noninoculated leaves was suppressed over extended incubation periods. The observation that phloem parenchyma or companion cells were infected in inoculated V20 leaves suggests that the restriction occurs after the phloem entry point in the long-distance movement pathway. V20 plants may suppress movement of TEV-GUS from phloem companion cells to sieve elements, the structures that permit passive transport of virus over long distances. Alternatively, V20 may restrict reentry of TEV-GUS back into phloem companion cells from sieve elements at sites distal to initial infection foci.

The infection phenotype of TEV-GUS in V20 tobacco plants was strikingly similar to the infection phenotypes of two classes of TEV-GUS mutants in susceptible Havana425 or Xanthi nc plants. Mutants that lack either the N- or C-terminal surface-exposed domain of CP are defective specifically in long-distance transport (12, 13). These domains consist of 29 and 18 amino acid residues, respectively, and contribute little, if at all, to virion assembly or stability (1, 12, 32). Mutants that contain alterations within the central region of HC-Pro also exhibit long-distance movement or systemic infection defects (3, 4, 9, 23). One long-distance movement-defective TEV-GUS mutant was shown to move into phloem parenchyma or companion cells of inoculated leaves (9). The HC-Pro mutants also possess other modest defects, such as reduced genome amplification, but the long-distance movement activity of HC-Pro appears to be a genetically distinct function (9, 22). Primarily on the basis of the fact that the TEV-encoded factors required for cell-to-cell movement and long-distance movement are different, the hypothesis that the virus interacts with unique sets of host factors or structures for cell-to-cell and long-distance movement was proposed (9). The data presented here support this hypothesis, as the V20 line possesses genetic determinants that affect predominantly long-distance movement. A simple interpretation of these data is that V20 encodes putative host factors that fail to interact efficiently with TEV-GUS or virus-encoded proteins required specifically for long-distance movement. However, other explanations are also possible. For example, the V20 alterations may affect components involved in both cell-to-cell and long-distance movement, but these components can be functionally replaced by other cellular factors in nonphloem cells only. The V20 restriction could also be due to a quantitative effect, such as a limiting host factor in all cells but with the effect more pronounced in cells associated with loading or unloading sieve elements. Alternatively, the restriction could conceivably be due to induction of a strain-specific resistant state in the systemic tissue. The nature of this resistance would require mechanisms that differ from those of known induced resistance systems, such as systemic acquired resistance (24, 34).

The genetic basis for the V20 restriction is more complex than can be explained by a single-gene model. Statistical analysis of phenotypes in F_2 progeny from the V20 × Havana425 cross suggests that the restriction of TEV-GUS to initial infection foci involves two nonlinked recessive loci. Several intermediate-susceptibility phenotypes were also observed among the segregants, and these are most easily explained by combinations of dominant and recessive alleles at either putative locus. Predicting a genotype that corresponds with these intermediate phenotypes, however, is not possible with the segregation analysis presented here. It should be noted that other plant lines with recessive mutations or alleles that appear to specifically restrict long-distance movement of TEV or other viruses have been identified. For example, cowpea chlorotic mottle bromovirus is able to establish infection in and move cell to cell through inoculated leaves of soybeans carrying two recessive genes derived from line PI346304, but entry into vascular tissue is restricted (16, 17). While recessive genes that condition these phenotypes are valuable as tools to dissect the different requirements for cell-to-cell and long-distance movement, they also have high practical value as sources of resistance in agricultural crops.

ACKNOWLEDGMENTS

We thank Patricia Valdez and Aaron Unterbrink for assistance with growing plants, Kate VandenBosch and Gyung Hee Lee for assistance with histochemical techniques, and Kristin Kasschau and Sunita Mahajan for helpful comments on the manuscript.

This research was supported by the U.S. Department of Agriculture (National Research Initiative Competitive Grants 91-37303-6435 and 95-37303-1867 to J.C.C.) and a National Research Service Award (AI09121 to M.C.S.) from the National Institutes of Health.

REFERENCES

1. **Allison, R. F., W. G. Dougherty, T. D. Parks, L. Willis, R. F. Johnston, M. Kelly, and F. B. Armstrong.** 1985. Biochemical analysis of the capsid protein gene and capsid protein of tobacco etch virus: N-terminal amino acids are located on the virion's surface. Virology **147:**309–316.
2. **Ammar, E. D., U. Järlfors, and T. P. Pirone.** 1994. Association of potyvirus helper component protein with virions and the cuticle lining the maxillary food canal and foregut of an aphid vector. Phytopathology **84:**1054–1060.
3. **Atreya, C. D., P. L. Atreya, D. W. Thornbury, and T. P. Pirone.** 1992. Site-directed mutations in the potyvirus HC-PRO gene affect helper component activity, virus accumulation, and symptom expression in infected tobacco plants. Virology **191:**106–111.
4. **Atreya, C. D., and T. P. Pirone.** 1993. Mutational analysis of the helper component-proteinase gene of a potyvirus: effects of amino acid substitutions, deletions, and gene replacement on virulence and aphid transmissibility. Proc. Natl. Acad. Sci. USA **90:**11919–11923.
5. **Bradford, M. M.** 1976. A rapid and sensitive method for the quantitation of microgram quantities of protein utilizing the principle of protein-dye binding. Anal. Biochem. **72:**248–254.
6. **Carrington, J. C., and D. D. Freed.** 1990. Cap-independent enhancement of translation by a plant potyvirus 5′ nontranslated region. J. Virol. **64:**1590–1597.
7. **Christie, S. R., D. E. Purcifull, and C. E. Dean.** 1974. Resistance in V20 tobacco to tobacco etch virus. Plant Dis. Rep. **58:**658–659.
8. **Citovsky, V., and P. Zambryski.** 1991. How do plant virus nucleic acids move through intercellular connections? Bioessays **13:**373–379.
9. **Cronin, S., J. Verchot, R. Haldeman-Cahill, M. C. Schaad, and J. C. Carrington.** 1995. Long-distance movement factor: a transport function of the potyvirus helper component-proteinase. Plant Cell **7:**549–559.
10. **Deom, C. M., M. Lapidot, and R. N. Beachy.** 1992. Plant virus movement proteins. Cell **69:**221–224.
11. **Ding, X. S., M. H. Shintaku, S. A. Arnold, and R. S. Nelson.** 1995. Accumulation of mild and severe strains of tobacco mosaic virus in minor veins of tobacco. Mol. Plant-Microbe Interact. **8:**32–40.
12. **Dolja, V. V., R. Haldeman, N. L. Robertson, W. G. Dougherty, and J. C. Carrington.** 1994. Distinct functions of capsid protein in assembly and movement of tobacco etch potyvirus in plants. EMBO J. **13:**1482–1491.
13. **Dolja, V. V., R. Haldeman-Cahill, A. E. Montgomery, K. A. VandenBosch, and J. C. Carrington.** 1995. Capsid protein determinants involved in cell-to-cell and long distance movement of tobacco etch potyvirus. Virology **207:**1007–1016.
14. **Dolja, V. V., H. J. McBride, and J. C. Carrington.** 1992. Tagging of plant potyvirus replication and movement by insertion of β-glucuronidase into the viral polyprotein. Proc. Natl. Acad. Sci. USA **89:**10208–10212.
15. **Gal-On, A., I. Kaplan, M. J. Roossinck, and P. Palukaitis.** 1994. The kinetics of infection of zucchini squash by cucumber mosaic virus indicate a function for RNA 1 in virus movement. Virology **205:**280–289.
16. **Goodrick, B. J., C. W. Kuhn, and H. R. Boerma.** 1991. Inheritance of nonnecrotic resistance to cowpea chlorotic mottle virus in soybean. J. Hered. **87:**512–514.
17. **Goodrick, B. J., C. W. Kuhn, and R. S. Hussey.** 1991. Restricted systemic movement of cowpea chlorotic mottle virus in soybean with nonnecrotic resistance. Phytopathology **81:**1426–1431.
18. **Holt, C. A., R. A. J. Hodgson, F. A. Coker, R. N. Beachy, and R. S. Nelson.** 1990. Characterization of the masked strain of tobacco mosaic virus: identification of the region responsible for symptom attenuation by analysis of an infectious cDNA clone. Mol. Plant-Microbe Interact. **3:**417–423.
19. **Hull, R.** 1991. The movement of viruses within plants. Semin. Virol. **2:**89–95.
20. **Ishikawa, M., S. Naito, and T. Ohno.** 1993. Effects of the *tom1* mutation of *Arabidopsis thaliana* on the multiplication of tobacco mosaic virus RNA in protoplasts. J. Virol. **67:**5328–5338.
21. **Jefferson, R. A.** 1987. Assaying chimeric genes in plants: the GUS gene fusion system. Plant Mol. Biol. Rep. **5:**387–405.
22. **Kasschau, K. D., and J. C. Carrington.** 1995. Unpublished observations.
23. **Klein, P. G., R. R. Klein, E. Rodríguez-Cerezo, A. G. Hunt, and J. G. Shaw.** 1994. Mutational analysis of the tobacco vein mottling virus genome. Virology **204:**759–769.
24. **Kuc, J.** 1982. Induced immunity to plant disease. BioScience **32:**854–860.
25. **Leisner, S. M., and R. Turgeon.** 1993. Movement of virus and photoassimilate in the phloem: a comparative analysis. Bioessays **15:**741–748.
26. **Li, X. H., and J. C. Carrington.** 1995. Complementation of tobacco etch potyvirus mutants by active RNA polymerase expressed in transgenic cells. Proc. Natl. Acad. Sci. USA **92:**457–461.
27. **Lucas, W. J., and R. L. Gilbertson.** 1994. Plasmodesmata in relation to viral movement within leaf tissues. Annu. Rev. Phytopathol. **32:**387–411.
28. **Negrutiu, I., R. Shillito, I. Potrykus, G. Biasini, and F. Sala.** 1987. Hybrid genes in the analysis of transformation conditions. 1. Setting up a simple method for direct gene transfer in plant protoplasts. Plant Mol. Biol. **8:**363–373.
29. **Restrepo, M. A., D. D. Freed, and J. C. Carrington.** 1990. Nuclear transport of plant potyviral proteins. Plant Cell **2:**987–998.
30. **Restrepo-Hartwig, M. A., and J. C. Carrington.** 1994. The tobacco etch potyvirus 6-kilodalton protein is membrane-associated and involved in viral replication. J. Virol. **68:**2388–2397.
31. **Schaad, M. C., and J. C. Carrington.** 1995. Unpublished observations.
32. **Shukla, D. D., P. M. Strike, S. L. Tracy, K. H. Gough, and C. W. Ward.** 1988. The N and C termini of the coat proteins of potyviruses are surface-located and the N terminus contains the major virus-specific epitopes. J. Gen. Virol. **69:**1497–1508.
33. **Traynor, P., B. M. Young, and P. Ahlquist.** 1991. Deletion analysis of brome mosaic virus 2a protein: effects on RNA replication and systemic spread. J. Virol. **65:**2807–2815.
34. **Uknes, S. J., K. Lawton, E. Ward, T. Gaffney, L. Friedrich, D. Alexander, R. Goodman, J.-P. Metraux, H. Kessmann, P. Ahl-Goy, M. GutRella, and J. Ryals.** 1993. The molecular biology of systemic acquired resistance, p. 1–10. *In* P. Gresshoff (ed.), Plant responses to the environment. CRC Press, Boca Raton, Fla.
35. **Verchot, J., and J. C. Carrington.** 1995. Debilitation of plant potyvirus infectivity by P1 proteinase-inactivating mutations and restoration by second-site modifications. J. Virol. **69:**1582–1590.
36. **Verchot, J., and J. C. Carrington.** 1995. Evidence that the potyvirus P1 protein functions as an accessory factor for genome amplification. J. Virol. **69:**3668–3674.
37. **Weiland, J. J., and M. C. Edwards.** 1994. Evidence that the αa gene of barley stripe mosaic virus encodes determinants of pathogenicity to oat (*Avena sativa*). Virology **201:**116–126.

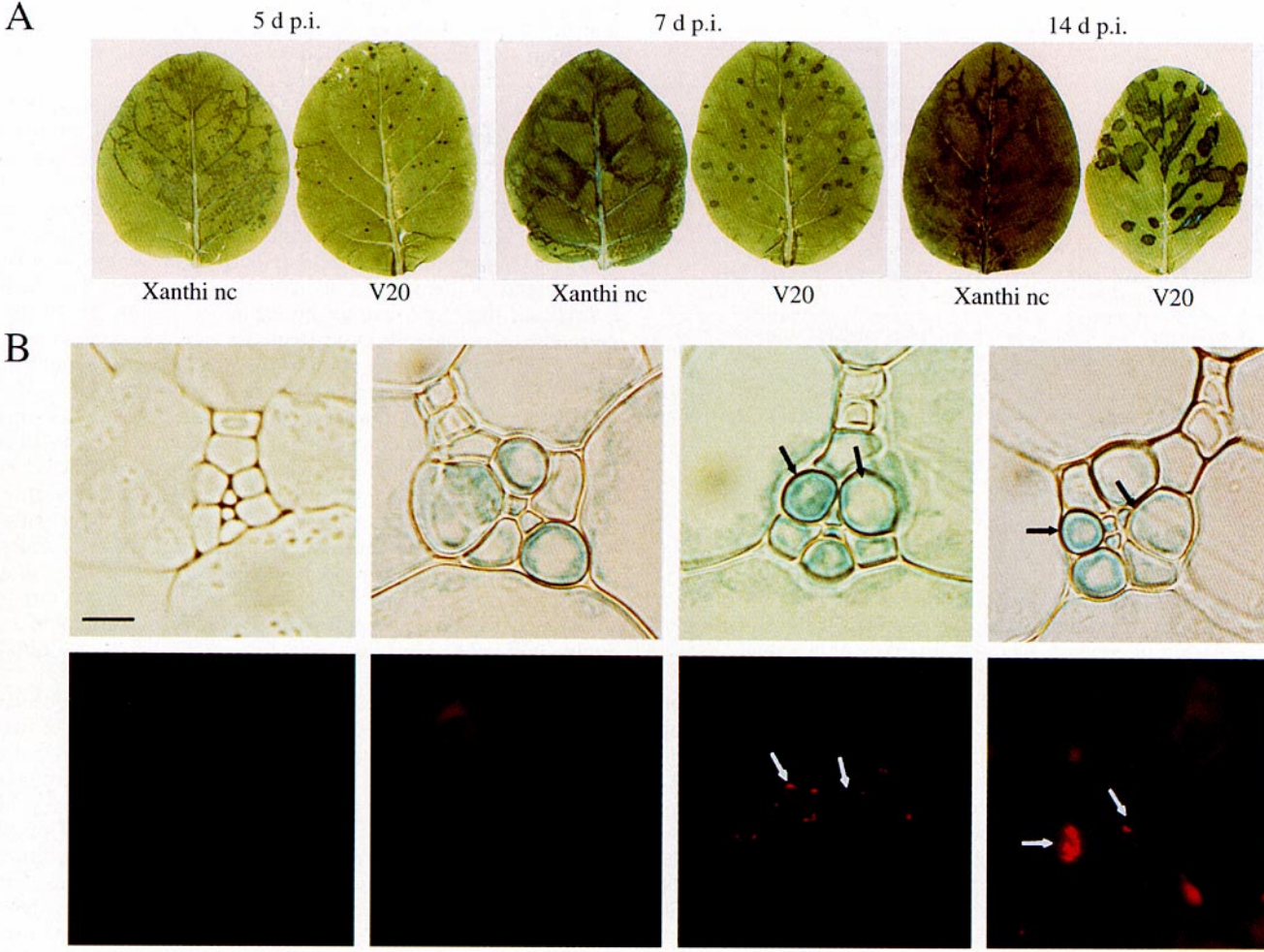
A
5 d p.i.
7 d p.i.
14 d p.i.
Xanthi nc
V20
Xanthi nc
V20
Xanthi nc
V20
B
Plant:
Antibody :
Non-infected V20
α-Capsid
Infected V20
Preimmune
Infected V20
α-Capsid
Infected Havana425
α-Capsid